Steady Convection in Stratified Fluid

By
Kenneth E. Heikes

Department of Atmospheric Science
Colorado State University
Fort Collins, Colorado

Colorado
State
University

Department of
Atmospheric Science

Paper No. 177

STEADY CONVECTION IN STRATIFIED FLUID

by

Kenneth E. Heikes

Department of Atmospheric Science
Colorado State University
Fort Collins, Colorado

February 1972

Atmospheric Science Paper No. 177

ABSTRACT

A linear theory is given for the case of steady thermal
convection in a stratified fluid with a general thermal
boundary condition at the upper and lower limits of the
system. The theory is applied to a number of fluid systems
and the results are discussed in terms of the Rayleigh num-
ber, the horizontal wave number and the vertical velocity
and temperature perturbation profiles in the vertical.

Kenneth E. Heikes
Atmospheric Science Department
Colorado State University
Fort Collins, Colo. 80521
November, 1971

ACKNOWLEDGEMENTS

TABLE OF CONTENTS

LIST OF TABLES

LIST OF FIGURES

LIST OF FIGURES--Continued

A_c Critical horizontal wave number scaled by the total depth of the system.

a Nondimensional horizontal wave number scaled by the lowest layer depth.

a_c Critical wave number. Value of a at the critical Rayleigh number.

α Coefficient of volume expansion at constant pressure.

β Vertical temperature gradient.

c Average height of a layer.

C_v Specific heat at constant volume.

C_p Specific heat at constant pressure.

d_i Thickness of layer i.

D Nondimensional differential operator.

D_f Scale height of the variable of state f.

∇ Del operator.

ε A number much less than one.

$\varepsilon_{\alpha_{i+1}}$ Ratio of α in layer i to that in layer i+1.

$\varepsilon_{\beta_{i+1}}$ Ratio of β in layer i+1 to that in layer i.

$\varepsilon_{K_{i+1}}$ Ratio of K in layer i+1 to that in layer i.

$\varepsilon_{\rho_{i+1}}$ Ratio of ρ_m in layer i+1 to that in layer i.

$\varepsilon_{\nu_{i+1}}$ Ratio of ν in layer i+1 to that in layer i.

ε^1_{i+1} $\varepsilon_{\rho_{i+1}} \cdot \varepsilon_{\nu_{i+1}}$

ε^2_{i+1} $\varepsilon_{\nu_{i+1}} / \varepsilon_{\alpha_{i+1}}$

ε^3_{i+1} $\varepsilon_{K_{i+1}}$

f	Variable of state.
f_m	Space average of f in a given layer.
g	Gravitational constant.
γ_B	Biot number at the bottom boundary.
γ_T	Biot number at the top boundary.
h_i	Height of the top of layer i.
$ht_{W_{max}}$	Nondimensional height at which the maximum vertical velocity occurs.
K	Thermometric conductivity ($=k/\rho_m C_p$).
k	Thermal conductivity.
k	Horizontal wave number.
$\bar{k}$	Unit vector in z direction.
k_x	Wave number in the x direction.
k_y	Wave number in the y direction.
∇^2	Laplacian operator.
μ	Coefficient of dynamic viscosity.
ν	Coefficient of kinematic viscosity.
p	Pressure.
P	Prandtl number.
Q	Radiative heat source.
R	Rayleigh number.
R_c	Critical Rayleigh number.
ρ	Density.
σ	Time constant.
t	Time.
T	Temperature.
T'	Temperature perturbation.

$\bar{v}$ Velocity vector.

w Vertical velocity, $w' = w'(x,y,z,t)$.

W' Vertical velocity, $W' = W'(z)$.

W Vertical velocity, $W = W(\zeta)$.

z Dimensional vertical coordinate.

ζ Nondimensional vertical coordinate.

I. INTRODUCTION

The phenomenon of thermal convection was first recog-
nized by Count Rumford in 1797 when he noticed the motion of
dust particles within the fluid contained in a large ther-
mometer he was using in an experiment. The word "convection"
was suggested by William Prout in 1834 in accord with con-
duction and radiation to denote this mode of heat transfer.
Among the earliest experiments performed in convection were
those by Thompson (1882) and Bénard (1900). Bénard found
that a certain critical vertical temperature gradient is
necessary for convection to begin and that a regular array
of hexagonal stationary cells becomes apparent with the on-
set of convection. The first analytical investigation of the
problem was performed by Rayleigh (1916). Rayleigh showed
that the stability or instability of the fluid is determined
by a combination of parameters describing the fluid. A de-
finitive treatment of the linear convective theory is given
by Pellow and Southwell (1940). More recently, an excellent
presentation of the subject is given by Chandrasekhar (1961).
Linear theories for two layer, homogeneous systems (Gribov
and Gurevich, 1957, and Ogura and Kondo, 1970) and one layer
systems with a general thermal boundary condition (Sparrow,
Goldstein and Jonsson, 1964, and Sasaki, 1967) have been

developed. In this paper these two extensions of the class-
ical theory are combined into an N layer, inhomogeneous
system with a general thermal boundary condition.

In the classical Rayleigh theory, describing simple
Bénard convection, heating from below establishes a negative
temperature gradient throughout the depth of a homogeneous
fluid of infinite horizontal extent with perfectly conducting
boundaries at the upper and lower surfaces. This produces a
gravitationally unstable density configuration with fluid of
higher density situated above fluid of lower density. Con-
vective overturning, however, occurs only if the degree of
instability is such that this adverse temperature gradient
cannot be alleviated by conduction and the motions generated
by the resulting buoyant force cannot be suppressed by vis-
cous dissipation.

Thus, an important objective of the Rayleigh and other
convection problems is to determine the critical set of
parameters, describing the fluid system, for which convec-
tive motions can just be maintained. These critical parame-
ters are combined in one nondimensional number called the
critical Rayleigh number. Besides the critical Rayleigh
number, the linear convection theory also produces the rela-
tive values of vertical velocity, perturbation temperature,
pressure, etc. at various heights in the fluid and the hori-
zontal extent, although not the specific form, of the con-
vective cells.

This investigation deals with steady thermal convection in a stratified fluid with general thermal boundary conditions. It differs from the idealized Bénard system in two ways. Unlike the perfect conductor thermal boundary condition assumed for the Bénard system, the thermal boundary condition in this case permits non-zero temperature perturbations at the boundaries due to a specified heat exchange with the environment surrounding the system. The second difference is that the convective motion generated in an unstable layer is free to penetrate other layers in the system. An individual layer, layer i, is defined by its mean temperature, T_{m_i}, temperature gradient, β_i, thickness, d_i, thermometric conductivity, K_i, kinematic viscosity, ν_i, and mean density, ρ_{m_i}. Like the Rayleigh theory, only the case of marginal stability with steady convective motions is considered.

It is necessary to specify for study a few of the many possible configurations of the system allowed by variations of the parameters describing individual layers, the number of layers and variations of the thermal boundary condition at the upper and lower boundaries of the system. In this paper, convection is examined in the following systems: (1) In a three layer system, in one case, the thickness of the top layer is varied and, in a second case, the thickness of the middle layer, for three different temperature gradients in the top layer, is varied; (2) In the three layer system, the thermal boundary condition at the lower surface

is varied from a perfect insulator to perfect conductor; and
(3) In a four layer system, the conductivity and viscosity
of the second layer above the ground are varied.

The theory described in this investigation was developed
with the intent of gaining a better understanding of convec-
tion in the presence of a temperature inversion and the
effect of certain fluid parameters upon steady convection.
Its application to various systems described in this paper
was motivated by interest in making the linear theory more
relevant to actual geophysical phenomena--specifically, con-
vection in the lower atmosphere. In natural convective phe-
nomena, the region of convection is often stratified, with
some layers being more stable than others. Also, in real
convective systems, the upper and lower surfaces of the con-
vective region do not approach the condition of being per-
fect conductors.

II. GOVERNING EQUATIONS

The general equations governing this problem are the equations of conservation of momentum, mass and energy and an equation of state. The following development of the basic equations follows closely that of Spiegal and Veronis (1960). The equations are given for a Cartesian coordinate system (x,y,z) in which gravity acts in the negative z direction. The three Navier-Stokes equations expressing conservation of momentum for a compressible viscous fluid are

$$\rho(\frac{\partial \bar{v}}{\partial t} + \bar{v} \cdot \nabla \bar{v}) = -\nabla p - g\rho \bar{k} + \mu [\nabla^2 \bar{v} + \frac{1}{3}\nabla(\nabla \cdot \bar{v})] \tag{1}$$

where the dynamic coefficient of viscosity, μ, is taken as constant. Conservation of mass is given by the continuity equation

$$\frac{\partial \rho}{\partial t} + \bar{v} \cdot \nabla \rho = -\rho \nabla \cdot \bar{v}. \tag{2}$$

The energy equation is

$$\rho C_v (\frac{\partial T}{\partial t} + \bar{v} \cdot \nabla T) + p \cdot \nabla \bar{v} = k\nabla^2 T + Q \tag{3}$$

$$+ \mu [\nabla \cdot (\bar{v} \cdot \nabla \bar{v}) - \frac{2}{3}(\nabla \cdot \bar{v})^2]$$

where Q is a radiational heat source and k is the thermal conductivity, taken as constant. It is shown by Spiegal and Veronis that the viscous dissipation terms in the energy balance, $\mu [\nabla \cdot (\bar{v} \cdot \nabla \bar{v}) - \frac{2}{3}(\nabla \cdot \bar{v})^2]$ are negligible compared to

the convection of internal energy. The equation of state is of the form

$$\rho = \rho(p,T) \quad . \tag{4}$$

These equations form a closed set of six equations and six unknowns: the three components of $\bar{v}$, p, T and ρ.

Each of the dependent variables in equations (1)-(4) may be expressed in terms of a deviation from the corresponding value in a quiescent, horizontally homogeneous reference atmosphere without radiational heat sources. The reference atmosphere is necessarily polytropic with constant lapse rate of temperature in each layer (Calder, 1967). The state variables, in the presence of convective motions, may be expressed as

$$f(x,y,z,t) = f_m + f_0(z) + f^1(x,y,z,t) \tag{5}$$

where f_m is the constant space average of f, f_0 is the vertical variation in the reference atmosphere and f^1 is a motion induced fluctuation.

The basic approximation to be applied, part of the Boussinesq approximation, is that the thickness, d, of any layer is much less than the smallest scale height of that layer. In terms of the density, this means that $d \ll D_\rho$ where D_ρ is the density scale height. Equivalently, the maximum density variation across a layer is much less than the mean density. Then if $\nabla \rho_0$ is the maximum density variation across a given layer,

$$\frac{\nabla \rho_0}{\rho_m} \equiv \varepsilon \ll 1 \quad . \tag{6}$$

An equation of state may be formulated by expanding ρ in a Taylor series about ρ_m. To the order ε, ρ may be expressed by

$$\rho = \rho_m[1 - \frac{T-T_m}{T_m} + \frac{p-p_m}{p_m}]$$

$$= \rho_m[1 - \alpha(T-T_m) + K(p-p_m)]$$

where

$$\alpha = \frac{1}{T_m} \quad \text{and} \quad K = \frac{1}{p_m} \quad .$$

This implies that

$$\rho_0 = \rho_m(Kp_0 - \alpha T_0) \tag{7}$$

and

$$\rho^1 = \rho_m(Kp^1 - \alpha T^1) \quad . \tag{8}$$

There are no motions in the basic state of this atmosphere. From equation (1), with no motions present

$$\frac{\partial p_0}{\partial z} = -g(\rho_m + \rho_0) \quad . \tag{9}$$

Subtracting this from equation (1), in the presence of thermally induced motions,

$$\rho(\frac{\partial \bar{v}}{\partial t} + \bar{v} \cdot \nabla \bar{v}) = \nabla p^1 - g\rho^1 \bar{k} + \mu[\nabla^2 \bar{v} + \frac{1}{3} \nabla(\nabla \cdot \bar{v})] \quad . \tag{10}$$

Substituting equations (5) and (6) into the continuity equation,

$$\nabla \cdot \bar{v} = -(\frac{\partial}{\partial t} + \bar{v} \cdot \nabla)(\varepsilon\frac{\rho_0}{\nabla\rho_0} + \varepsilon\frac{\rho^1}{\nabla\rho_0}) - (\varepsilon\frac{\rho_0}{\nabla\rho_0} + \varepsilon\frac{\rho^1}{\nabla\rho_0})\nabla \cdot \bar{v} \tag{11}$$

To the order ε, equations (10) and (11) are, respectively,

$$\frac{\partial \bar{v}}{\partial t} + \bar{v} \cdot \nabla \bar{v} = -\frac{1}{\rho_m} \nabla p' - g \, \varepsilon \frac{\rho^1}{\nabla \rho_0} \bar{k} + \nu \nabla^2 \bar{v} \ . \tag{12}$$

and

$$\nabla \cdot \bar{v} = 0 \ . \tag{13}$$

The term $g\varepsilon \frac{\rho^1}{\nabla \rho_0} \bar{k}$ has been retained in spite of the factor ε because convection could not occur without this buoyancy term. Inclusion of this term implies that characteristic accelerations within the fluid are of a much smaller magnitude than the gravitational acceleration.

The next approximation imposed, the second part of the Boussinesq approximation, is that density fluctuations are entirely the result of motion-induced temperature fluctuations. The validity of this approximation is demonstrated by equation (12) where it is noted that p' is of $O(\varepsilon)$ compared to the density fluctuation. Equation (8) may then be written

$$\rho' = -\rho_m \alpha T' \ . \tag{14}$$

The immediate consequence of this approximation may be seen in the momentum equation, equation (12) which becomes

$$\frac{\partial \bar{v}}{\partial t} + \bar{v} \cdot \nabla \bar{v} = -\frac{1}{\rho_m} \nabla p' + g\alpha T' \bar{k} + \nu \nabla^2 \bar{v} \ . \tag{15}$$

If there exist no radiative sources or sinks of energy within the fluid, in the absence of motion

$$k \nabla^2 T_0 = 0 \ . \tag{16}$$

The perturbation energy equation, neglecting the viscous dissipation terms, then becomes

$$\rho_m C_v (\frac{\partial T'}{\partial t} + \bar{v}\cdot\nabla T) + p\nabla\cdot\bar{v} = k\nabla^2 T' \ . \tag{17}$$

Here, although $\nabla\cdot\bar{v}\approx o$, p is large enough that $p\nabla\cdot\bar{v}$ is of about the same magnitude as the other terms in the equation. Using equations (7), (11) and (14), $p\nabla\cdot\bar{v}$ may be written approximately as

$$p\nabla\cdot\bar{v} = p_m(\frac{\partial}{\partial t} + \bar{v}\cdot\nabla)(\frac{T_0+T'}{T_m} - \frac{p_0}{p_m})$$

which reduces to

$$p\nabla\cdot\bar{v} = \frac{p_m}{T_m}(\frac{\partial}{\partial t} + \bar{v}\cdot\nabla)(T_0 + T') + w'g\rho_m \ .$$

Incorporating this result in equation (17),

$$\rho_m C_p (\frac{\partial T'}{\partial t} + \bar{v}\cdot\nabla T) + w'g\rho_m = k\nabla^2 T'$$

or

$$(\frac{\partial T'}{\partial t} + \bar{v}\cdot\nabla T') + w'(\frac{\partial T_0}{\partial z} + g/C_p) = K\nabla^2 T' \tag{18}$$

where $K = k/\rho_m C_p$ is the thermometric conductivity and g/C_p is the adiabatic temperature gradient.

In summary, the complete set of approximate equations governing thermal convection in a compressible fluid are equations (12), (14), (15) and (18). The equivalent equations for an incompressible fluid may be written by replacing $\frac{\partial T_0}{\partial z} + \frac{g}{C_p}$, where $\frac{\partial T_0}{\partial z}$ is the temperature gradient excess over the adiabatic lapse, $\frac{g}{C_p}$, by $\beta = -\frac{\partial T_0}{\partial z}$, where β is the

temperature lapse rate in an incompressible fluid and by replacing C_p with C_v. The equations for an incompressible fluid have been adopted here to facillitate comparison of this work to that done by other authors.

Mihaljan (1962) suggests that the Boussinesq approximations probably have greater validity in the thermodynamic equations than the mechanical equations. He also demonstrates that the Boussinesq system is incomplete for describing the energetics because it neglects the term necessary to describe the rate at which work is done by the hydrostatic pressure through the divergence field in the conversion of internal to potential energy. Thus, any discussion of the energetics of the linear stability theory is only of a heuristic nature.

III. METHOD OF SOLUTION

Assuming that convection first occurs as an infinitesimal perturbation on the initial, quiescent fluid, the perturbation equations describing the onset of convection are given by equations (13), (14), (15) and (18) after neglecting products of perturbation quantities. The perturbation equations relative to an incompressible fluid are then

$$\nabla \cdot \bar{v} = 0 , \tag{19}$$

$$\rho' = -\rho_m \alpha T' , \tag{20}$$

$$\frac{\partial \bar{v}}{\partial t} = -\frac{1}{\rho_m} \nabla p' + g \alpha T' \bar{k} + \nu \nabla^2 \bar{v} , \tag{21}$$

and

$$\frac{\partial T'}{\partial t} - w' \beta = K \nabla^2 T' \tag{22}$$

where all primed quantities are perturbations of infinitesimal amplitude.

From equations (19) and (21), eliminating p', we obtain

$$\frac{\partial}{\partial t} \nabla^2 w' = g \alpha \left(\frac{\partial^2}{\partial x^2} + \frac{\partial^2}{\partial y^2} \right) T' + \nu \nabla^4 w' . \tag{23}$$

Taking the divergence of equation (21), results in

$$-\frac{1}{\rho_m} \nabla^2 p' + g \alpha \frac{\partial T'}{\partial z} = 0 . \tag{24}$$

Differentiating the z component of equation (21) with respect to z, produces

$$\frac{\partial}{\partial t}(\frac{\partial w'}{\partial z}) = - \frac{1}{\rho_m} \frac{\partial^2 p'}{\partial z^2} + g\alpha\frac{\partial T'}{\partial z}\bar{k} + \nu\nabla^2\frac{\partial w'}{\partial z} . \qquad (25)$$

Equations (22), (24) and (25) will be useful in deriving the boundary conditions at the interfaces between layers. Eliminating T' from equations (22) and (23) results in a sixth order differential equation in w'

$$[P\frac{\partial}{\partial t} - (\frac{\partial^2}{\partial^2 z} - \nabla_1^2)][\frac{\partial}{\partial t} - (\frac{\partial^2}{\partial z^2} - \nabla_1^2)](\frac{\partial^2}{\partial z^2} - \nabla_1^2) \ w' = g\frac{\alpha\beta}{k\nu}\nabla_1^2 w'$$

$$(26)$$

where P in the Prantdl number, $P = K/\nu$ and $\nabla_1^2 = \frac{\partial^2}{\partial x^2} + \frac{\partial^2}{\partial y^2}$.

The analysis is made by assuming horizontally periodic solutions of a specified wave number and with an exponential time dependence. Including an unspecified z dependence, all perturbation quantities may be expressed by

$$X(x,y,z,t) = X(z) \ \exp[i(k_x x + k_y y) + \sigma t] \qquad (27)$$

where σ is, in general, complex. However, for the case of marginal, or neutral, stability, in which convective motions are not damped out but just sustain themselves, the real part of σ must be zero since the perturbation neither amplifies nor dies in time. The imaginary part of σ may be either zero or non-zero. If it is not zero, the marginal state is said to be overstable and the convective motions are oscillatory. If the imaginary part of σ is zero, the principle of the exchange of stabilities is valid and the motions in the fluid are steady and take the form of stationary convective cells. The principle of the exchange of

stabilities is assumed here and thus the study is limited to that of steady convective motions.

Assuming $\sigma = 0$, equation (27) becomes

$$X = X(z) \exp[i(k_x x + k_y y)]$$

In particular, the vertical velocity, w', and the temperature and pressure perturbations, T' and p', may be written

$$\begin{bmatrix} w' \\ T' \\ p' \end{bmatrix} = \begin{bmatrix} W'(z) \\ T'(z) \\ p'(z) \end{bmatrix} \exp[i(k_x x + k_y y)] \quad .$$

(28a)
(28b)
(28c)

For functions with this dependence on x, y and t,

$$\frac{\partial}{\partial t} = 0, \quad V_1^2 = -(k_x^2 + k_y^2) = -k^2 \quad \text{and} \quad V^2 = \frac{\partial^2}{\partial z^2} - k^2 \quad (29)$$

where

$$k = \sqrt{k_x^2 + k_y^2} \quad .$$

Substituting equations (28) and (29) into equations (23), (24), (25) and (26), we get

$$(\frac{\partial^2}{\partial z^2} - k^2)^2 W' = \frac{g\alpha}{\nu} k^2 T' , \tag{30}$$

$$(\frac{\partial^2}{\partial z^2} - k^2) p' = \rho_m g\alpha \frac{\partial T'}{\partial z} , \tag{31}$$

$$-\frac{1}{\rho_m} \frac{\partial^2 p'}{\partial z^2} + g\alpha \frac{\partial T'}{\partial z} + \nu(\frac{\partial^2}{\partial z^2} - k^2)\frac{\partial w'}{\partial z} = 0 , \tag{32}$$

and

$$(\frac{\partial^2}{\partial z^2} - k^2)^3 W' = - g\frac{\alpha\beta}{K\nu} k^2 W' \tag{33}$$

where T' denotes $T'(z)$.

It is convenient to nondimenionalize equations (30)-(33), choosing for the unit of length the height of the lowest layer, h_1. The nondimensional height, ζ, vertical velocity, W, wave number, a, and differential operator, D^2, may then be expressed by

$$\zeta = z/h_1, \quad W = W'/h_1, \quad a = kh_1 \text{ and } D^2 = \frac{1}{h_1^2} \frac{\partial^2}{\partial z^2} \; .$$

Substituting these relations into equations (30)-(33) gives

$$(D^2 - a^2)^2 W = g\frac{\alpha h_1^2}{\nu} a^2 T' , \qquad (34)$$

$$(D^2 - a^2)p' = \rho_m g\alpha h_1 DT' , \qquad (35)$$

$$- \frac{h_1}{\rho_m} D^2 p' + g\alpha h_1^2 DT' + \nu(D^2 - a^2)DW = 0 , \qquad (36)$$

and

$$(D^2 - a^2)^3 W = - Ra^2 W \qquad (37)$$

where R is the Rayleigh number, $R = g\frac{\alpha\beta}{k\nu} h_1^4$.

The solution to equation (37) in a given layer, layer i, may be written

$$W_i = \sum_{j=1}^{3} A_{ji} e^{q_{ji}(\zeta-c_i)} + B_{ji} e^{-q_{ji}(\zeta-c_i)} \qquad (38)$$

where the A_{ji} and B_{ji} must be determined from the boundary conditions and c_i is the average height of the layer for which W_i is a solution. The q_{ji} are roots of the differential equation, equation (37), and are given by

$$q_{1i} = a(\tau_i - 1)^{1/2}, \quad q_{2i} = Re(q_{2i}) + iIm(q_{2i}) \text{ and } q_{3i} = q_{2i}{}^{*}$$

where

$$\tau_i = (R_i/a^4)^{1/3},$$

$$Re(q_{2_i}) = a[\frac{1}{2}(1 + \tau_i + \tau_i^2)^{1/2} + \frac{1}{2}(1 + \frac{1}{2}\tau_i)]^{1/2},$$

and

$$Im(q_{2_i}) = a[\frac{1}{2}(1 + \tau_i + \tau_i^2)^{1/2} - \frac{1}{2}(1 + \frac{1}{2}\tau_i)]^{1/2}.$$

The superscript * denotes the complex conjugate. This par-
ticular form of solution (i.e., subtracting c_i from ζ) was
chosen so that for layers of large ζ the exponent of e would
not be extremely large, thus facilitating maximum computa-
tional accuracy. Equation (38) is applied to each layer in
the N layer system and the solutions at the interfaces be-
tween layers are matched. A schematic diagram of the system
and the parameters describing it is shown in Fig. 1.

Six boundary conditions for each layer are necessary to
solve for the A_{ji} and B_{ji} in all N layers. The boundary
conditions are all homogeneous and thus we have a homogeneous
problem for which the solution is given by the R_i and a
such that the determinant of the coefficient matrix of the
A_{ji} and B_{ji} is zero. The R_i are all related through the
parameters ϵ^1, ϵ^2 and ϵ^2 and therefore in designating R_1 one
specifies all R_i. Thus, given an a, we have an eigenvalue
problem in R_1. Physically, R is the ratio in a given layer
of the rate of viscous dissipation of kinetic to the rate of
buoyant release of internal energy in a unit vertical column.
Convective overturning begins for the lowest mode of a at

free

$$(D^2 - a^2)^3 W_N = -R_N a^2 W_N \qquad \text{Layer N}$$

$$\epsilon_N^1, \ \epsilon_N^2, \ \epsilon_N^3 \text{---} \qquad \text{Interface N}$$

$$(D^2 - a^2)^3 W_{N-1} = -R_{N-1} a^2 W_{N-1} \qquad \text{Layer N-1}$$

$$\epsilon_{N-1}^1, \ \epsilon_{N-1}^2, \ \epsilon_{N-1}^3 \text{---} \qquad \text{Interface N-1}$$

$$\epsilon_2^1, \ \epsilon_2^2, \ \epsilon_2^3 \text{---} \qquad \text{Interface 2}$$

$$(D^2 - a^2)^3 W_1 = -R_1 a^2 W_1 \qquad \text{Layer 1}$$
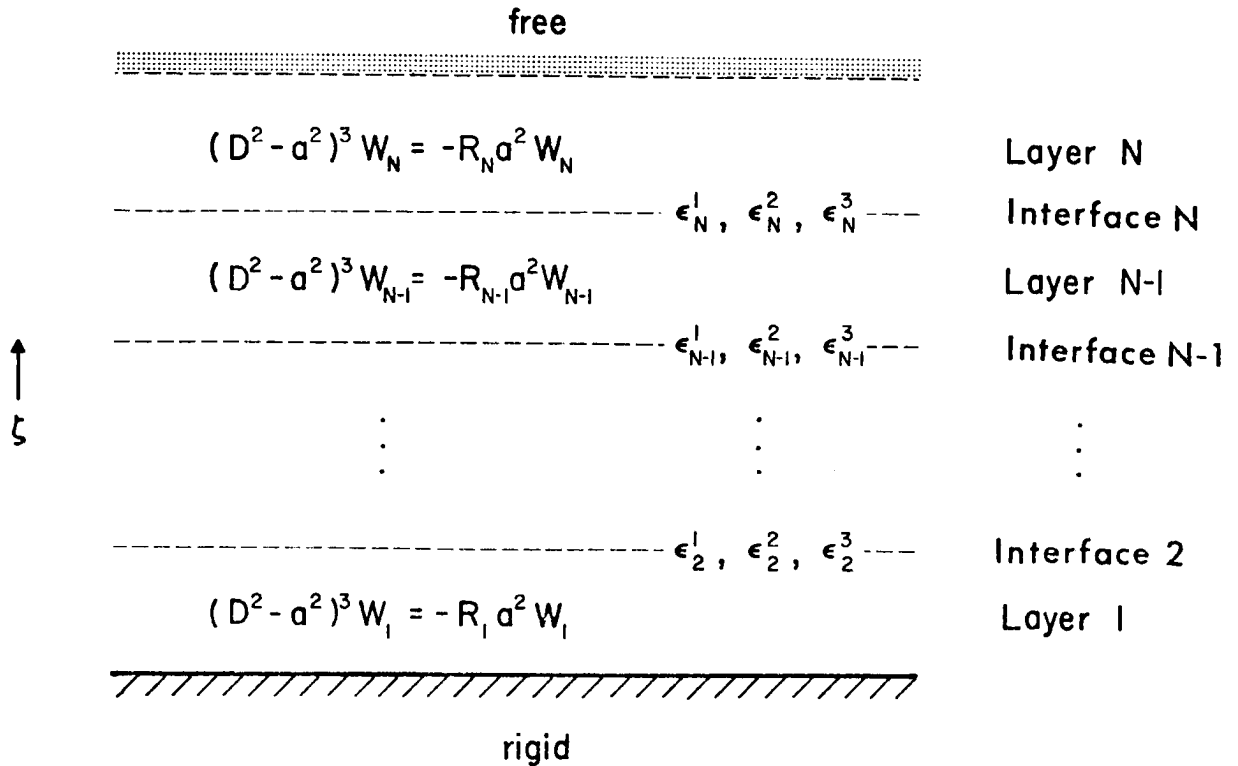
rigid

Fig. 1. The N layer system with a characteristic equation for each layer. The first interface is arbitrarily labeled "interface 2." The upper surface is free: the lower surface regid. Ratios of parameters between layers i and i+1 are given by ϵ_{i+1}^1, ϵ_{i+1}^2 and ϵ_{i+1}^3.

the minimum value of R_1. The minimum R and the value of a corresponding to that R are the critical Rayleigh number and critical wave number, R_c and a_c.

A description of the boundary conditions at the lower and upper surfaces and at each interface follows.

IV. BOUNDARY CONDITIONS

A. Lower Surface--Rigid.

At the lower surface u', v' and w' are required to be zero. Requiring u' and v' to be zero results in the rigid boundary condition. It implies, through the continuity equation, that $DW_i = 0$. Thus, at the lower surface

$$W_i = 0 \tag{39}$$

and

$$DW_i = 0 . \tag{40}$$

The thermal boundary condition is that the conductive heat flux, $- KDT'$, and perturbation temperature, T', are related by an arbitrary constant γ_B',

$$\frac{-KDT'}{T'} = \gamma_B'$$

or

$$(D + \gamma_B)T' = 0 \tag{41}$$

where γ_B is the so-called Biot number, γ_B'/K.

B. Upper Surface--Free.

Similarily, three boundary conditions exist at the upper surface. At the upper surface the vertical velocity and tangential stress are required to be zero. The zero tangential stress condition gives the free boundary condition $D^2W = 0$. Thus, we have

$$W = 0 \qquad (42)$$

and

$$D^2W = 0 \quad . \qquad (43)$$

The thermal boundary condition at the upper surface has the same form as that at the lower surface however the Biot constant, denoted by γ_T here, may be different. We have

$$(D + \gamma_T)T' = 0 \quad . \qquad (44)$$

C. Interface Boundary.

To satisfy the requirement of six N boundary conditions, it remains that there must be six boundary conditions at each interface between layers. These are continuity of vertical velocity, horizontal velocity, tangential stress, perturbation pressure, temperature and conductive heat flux. Continuity of vertical velocity at the interface between layers i and i+1 gives

$$W_i = W_{i+1} \quad . \qquad (45)$$

That the horizontal velocity be continuous across the interface implies through the continuity equation that

$$DW_i = DW_{i+1} \quad . \qquad (46)$$

Continuity of tangential stress yields

$$\mu_i(D^2 + a^2)W_i = \mu_{i+1}(D^2 + a^2)W_{i+1} \qquad (47)$$

or

$$(D^2 + a^2)W_i = \varepsilon'_{i+1}(D^2 + a^2)W_{i+1} \qquad (48)$$

where

$$\varepsilon^1_{i+1} = \frac{\rho_{m_{i+1}}}{\rho_{m_i}} \cdot \frac{\nu_{i+1}}{\nu_i} \quad .$$

From equations (35) and (36), we obtain the condition of continuity pressure in terms of W

$$(D^2 - a^2)DW_i = \varepsilon^1_{i+1}(D^2 - a^2)DW_{i+1} \quad . \tag{49}$$

Equation (34) yields the condition for continuity of perturbation temperature

$$(D^2 - a^2)^2 W_i = \varepsilon^2_{i+1}(D^2 - a^2)^2 W_{i+1} \tag{50}$$

where

$$\varepsilon^2_{i+1} = \frac{\alpha_i}{\alpha_{i+1}} \cdot \frac{\nu_{i+1}}{\nu_i} \quad .$$

Finally, continuity of conductive and convective heat flux is given by

$$-K_i DT_i' + \rho_{m_i} C_{v_i} (T_{m_i} - \beta_i \zeta h_1) W_i =$$

$$-K_{i+1} DT'_{i+1} + \rho_{m_{i+1}} C_{v_{i+1}} (T_{m_{i+1}} - \beta_{i+1} \zeta h_1) W_{i+1}$$

where $(T_{m_i} - \beta_i \zeta h_i) = (T_{m_{i+1}} - \beta_{i+1} \zeta h_i)$ is a property of the basic state and $W_i = W_{i+1}$. If $\rho_{m_{i+1}} C_{p_{i+1}} = \rho_{m_i} C_{p_i}$, which is assumed in this study, continuity of heat flux is given by

$$-K_i DT_i' = -K_{i+1} DT'_{i+1}$$

or, differentiating equation (34), we have

$$(D^2 - a^2)^2 DW_i = \varepsilon^2_{i+1} \varepsilon^3_{i+1} (D^2 - a^2)^2 DW_{i+1} \tag{52}$$

where

$$\varepsilon_3^{i+1} = \frac{K_{i+1}}{K_i} \quad .$$

The presence of the convective term in the perturbation heat flux boundary condition would require explicit inclusion of the mean state temperature field and the additional convective parameter, C_v.

V. DISCUSSION OF RESULTS

Before beginning the discussion of the application to various stratified systems, some general things which apply to all systems tested must be pointed out. One is that the lowest layer in each system has a gravitationally unstable density configuration resulting from a negative temperature gradient. In each case presented, the Rayleigh number discussed in the text always refers to the Rayleigh number of the lowest layer, R_1. The system being considered in a given section is defined in a table at the beginning of that section and is followed by a table of the more important critical Rayleigh and wave numbers versus the parameter being varied.

A. The Classical, Rigid-free Problem.

The model was first tested on the classical, rigid-free, Rayleigh problem and exact agreement was found. The classical values given by Chandrasekar (1961) are R_c = 1100.65 and a_c = 2.682. The values found in the present case are R_c = 1100.64961 and a_c = 2.68232. A graph of W and T' versus ζ is shown in Fig. 2 for the classical case. Since only relative values of W and T' within a given profile can be ascertained from this analysis (absolute values of W and T' cannot be found) each profile has been normalized so that the maximum value of W is 1.00.
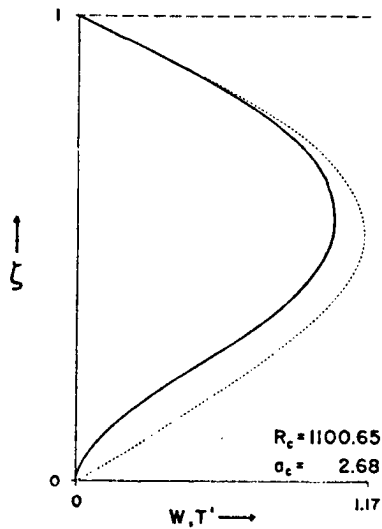
Fig. 2. Vertical velocity (solid) and temperature perturba-
tion (dotted) profiles for the classical, rigid-
free, Rayleigh problem.

B. In a Three Layer System, the Thickness of One Layer is
Varied.

The first investigation is an amplification of several

studies by authors who have considered the problem of con-

vection in a two layer system. Gribov and Gurevich (1957)

investigated the case of an unstable layer bordered either

above or below by a stable layer of infinite vertical extent.

Ogura and Kondo (1970) studied the effect of the stability

and depth of an upper stable or neutral layer for rigid-

rigid, rigid-free, and free-free dynamic boundary conditions.

Here the effect of a third layer is examined by first vary-

ing the thickness of the top layer (Part B.1.) and, second,

by varying the thickness of the middle layer (Part B.2.) for

three different stabilities of the top layer. A third layer

is important when convection exists in the presence of a temperature inversion because often fluid is distinguished by three distinct layers in that case.

B.1.   The Thickness of the Top Layer is Varied.

Table 1.   Parameters defining the system of Part B.1.

Interface i	ϵ_{α_i} ϵ_{β_i} ϵ_{K_i} ϵ_{ν_i} ϵ_{ρ_i}					Layer i	h_i
2	1	-1	1	1	1	1	1.0
3	1	-1	1	1	1	2	1.5
						3	variable

Thermal boundary condition: perfectly conducting boundaries, $\gamma \rightarrow \infty$.

Table 2.   Critical Rayleigh number and wave number relative to the lowest layer and critical wave number relative to the total depth, A_c.

h_3	R_c	a_c	$A_c(=a_c h_3)$
1.50	399.147	1.8688	2.8032
1.52	397.982	1.8574	2.8232
1.53	397.753	1.8584	2.8434
1.54	397.556	1.8480	2.8459
1.55	397.571	1.8441	2.8584
1.64	401.561	1.8268	2.9960
1.66	402.813	1.8263	3.0317
1.68	404.027	1.8267	3.0688
1.78	408.177	1.8316	3.2608
1.80	408.490	1.8321	3.2978
1.82	408.619	1.8319	3.3341
1.84	408.564	1.8312	3.3694
2.00	401.583	1.7980	3.5960
2.20	360.222	1.5873	3.4920
2.38	213.845	1.2339	2.9305
2.50	129.070	1.1319	2.8297
2.70	65.226	1.0246	2.7664

In Part B.1., the height of the top layer is increased from 1.5 to 2.7. This corresponds to the thickness of the top layer increasing from 0 to 1.2. The system is homogeneous throughout except for temperature gradient. A temperature inversion exists in the second layer with its temperature gradient of equal magnitude but opposite sign as that in the other two layers.

Addition of the third, unstable layer initially decreases the stability of the system as evidenced by decreasing critical Rayleigh number in Fig. 3 for h_3 = 1.50 to ~ 1.545. It is reasonable to expect that the system be more unstable when a larger proportion of it consists of unstable fluid. However, after h_3 = 1.545, R_c begins to increase, reaching a maximum at about h_3 = 1.82 and then decreases.

An explanation of this behavior of R_c is provided by inspection of the W and T' profiles for various values of h_3 and consideration of the effect of the upper boundary condition. Initially, R_c decreases because the restrictions imposed on the fluid motion in the lowest layer by the upper boundary condition are relaxed as the upper boundary moves away from the lowest layer.

The increase in R_c at about h_3 = 1.545 may be understood after examination of the W and T' profiles for h_3 = 1.50 and h_3 = 1.54 (Figure 4 a and b) where it is noted that a small region of negative temperature perturbation occupies the upper part of the fluid. The area and intensity of this
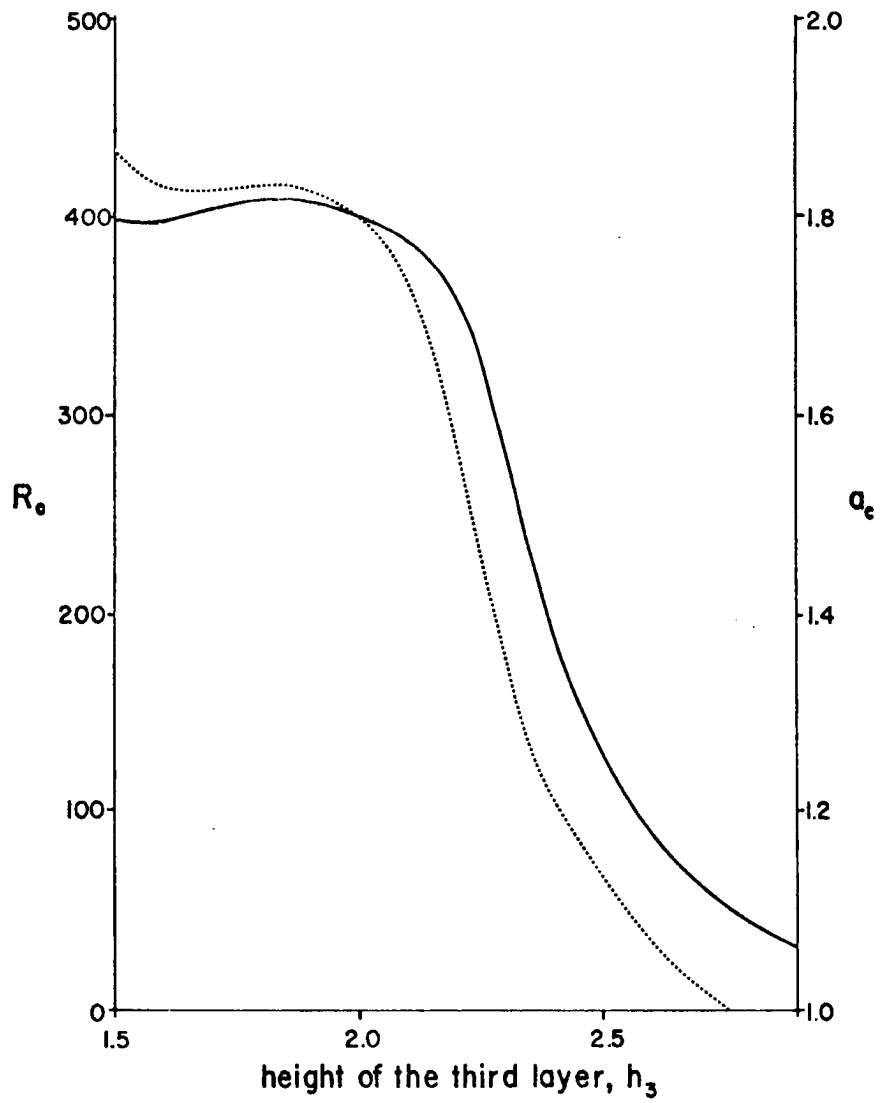
Fig. 3. Critical Rayleigh number (solid), R_c, and critical wave number (dotted), a_c, versus height of the third layer, h_3.

region increases for increasing h_3. Coupled with a positive vertical velocity, this region of negative temperature perturbation constitutes a part of the fluid undergoing forced convection where fluid cooler than its surroundings is being forced upward and some of the kinetic energy from the lower part of the fluid is being stored as potential energy in the upper layers. As stated previously, the critical Rayleigh number is the ratio of internal energy released by buoyancy to kinetic energy dissipated by viscosity per unit column of a fluid layer such that convective motions neither damp out nor amplify in time. Also, it must be remembered that we refer only to the critical Rayleigh number of the lowest layer. With these facts in mind, it is easy to understand that R_c increases because a larger rate of release of internal energy in layer one becomes necessary to generate sufficient kinetic energy to penetrate the entire depth of the system with increasing h_3. The reason more kinetic energy is needed is that an increasing amount of the kinetic energy goes to potential energy in the upper layers. At the same time the amount of kinetic energy dissipated in the first layer increases only slightly, if at all. Thus, R_c increases.

A local R_c maximum occurs at $h_3 = 1.82$ with the advent of a small region of free convection (WT'>0) at the top of the fluid (Fig. 4 c). Increasing the thickness of the third layer beyond this (Fig. 4 d, e and f) increases the relative magnitude of this new region of free convection and decreases
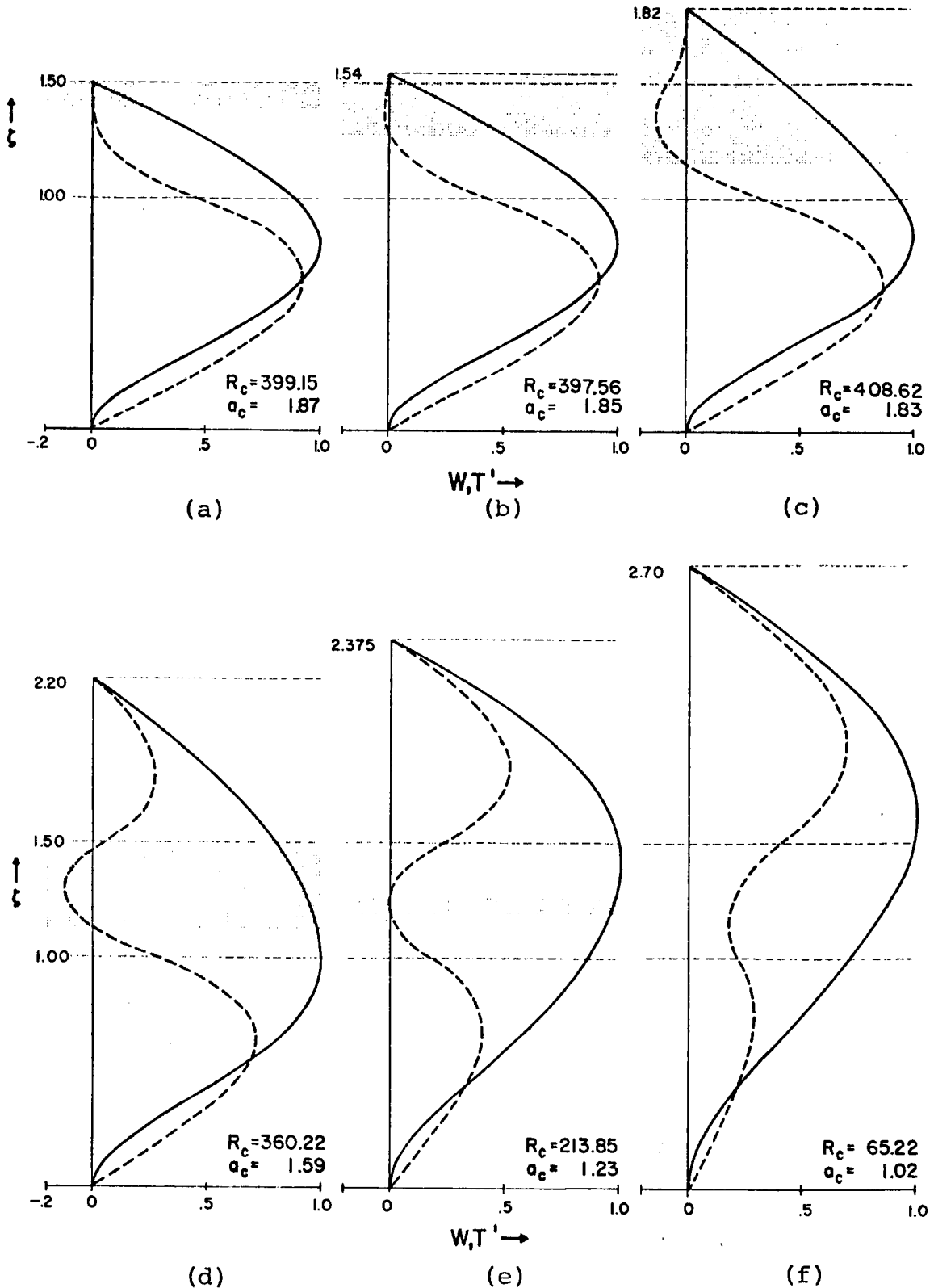
Fig. 4. Vertical velocity (solid), W, and temperature per-
turbation (dashed), T', for various values of top
layer thickness. Regions of forced convection are
shaded. Interfaces are shown by horizontal dashed
lines.

the region of forced convection. R_c decreases because an increasing amount of the internal energy, which generates the kinetic energy to drive the convective circulation of the entire system, is being released in the upper layer and therefore R_c, proportional to the rate of release of internal energy in the lowest layer, decreases. Also, less kinetic energy is lost to potential energy. After $h_3 = 1.82$, R_c decreases monotonically and, in the limit, R_c approaches zero as h_3 goes to infinity.

Physically, as the upper unstable layer occupies almost the entire depth of the system relative to layers one and two, the rates of release of internal energy in the lowest layer necessary to maintain the circulation there against viscous dissipation becomes very small because the circulation is mainly being driven by the third layer. Mathematically, the decreasing R_c may be explained as follows. Since the temperature gradients of the third and first layers are equal and since for large h_3 we may ignore layer two, the system approaches the classical, homogeneous Bénard system for large h_3. We may assume, therefore, that for large values of h_3 the critical Rayleigh number R_c' relative to the total depth of the fluid, h_3, is constant and equal to 1100.65 which is the value for the classical, rigid-free Rayleigh problem. We have

$$R_c' = g\frac{\alpha\beta}{k\nu}h_3^4 = 1100.65 \quad .$$

However, if the system is now scaled by h_1, equal to, for example, a tenth h_3 ($h_1 = \frac{h_3}{10}$), the critical Rayleigh number relative to the lowest layer is

$$R_c = g\frac{\alpha\beta}{k\nu}h_1^4 = g\frac{\alpha\beta}{k\nu}\left(\frac{h_3}{10}\right)^4 = 1100.65 \times 10^{-4} .$$

The reason for small R_c with h_3 large compared to h_1 is clear. The trend toward the classical case (Fig. 2) can be seen in Fig. 4 f.

Inspection of Table 1 and Fig. 3 shows that the critical horizontal wave number, a_c, versus h_3 has a response similar in form to that for R_c versus h_3. However, it reaches a local minimum before R_c arrives at its first minimum and a_c attains its maximum before R_c reaches its local maximum.

The horizontal extent of the convective cell, $2\pi/a$, relative to the lowest layer, first increases, then decreases, and finally increases indefinitely as h_3 goes to infinity. The reasons for the first minimum and then maximum of a_c are not clear. Apparently the most effective cell size is only indirectly dependent upon the fluid's stability. The final decrease of a_c may be explained by the fact that the system is essentially the classical, rigid-free system for large values of h_3. The horizontal extent of the convective cell in the classical system is constant relative to the total depth of the system (the total depth is h_3 in this case). Now, considering the cell relative to the lowest layer, which decreases in height relative to h_3 as h_3 increases,

the horizontal extent increases as h_3 increases. Thus, a_c decreases. Mathematically, A_c, the wave number relative to the total depth, h_3, for the classical case is

$$A_c = kh_3 = 2.682 \quad .$$

For $h_1 = h_3/10$, the corresponding wave number, a_c, relative to the lowest layer is

$$a_c = kh_3/10 = .2682 \quad .$$

Table 1 and Fig. 5 show that A_c tends to the limit $A_c = 2.682$, suggested in the previous paragraph, as h_3 increases beyond $h_3 = 2.07$. Fig. 4 also demonstrates that A_c suddenly begins to decrease at approximately the same value of h_3 for which the height of maximum vertical velocity, $ht_{W_{max}}$, begins to increase and penetrate the inversion layer. Thus, it appears that the cell size remains fairly constant relative to the lowest layer when the region of maximum velocity in the fluid is confined below the inversion. After the region of maximum velocity penetrates the inversion the cell size remains almost constant relative to the total depth.
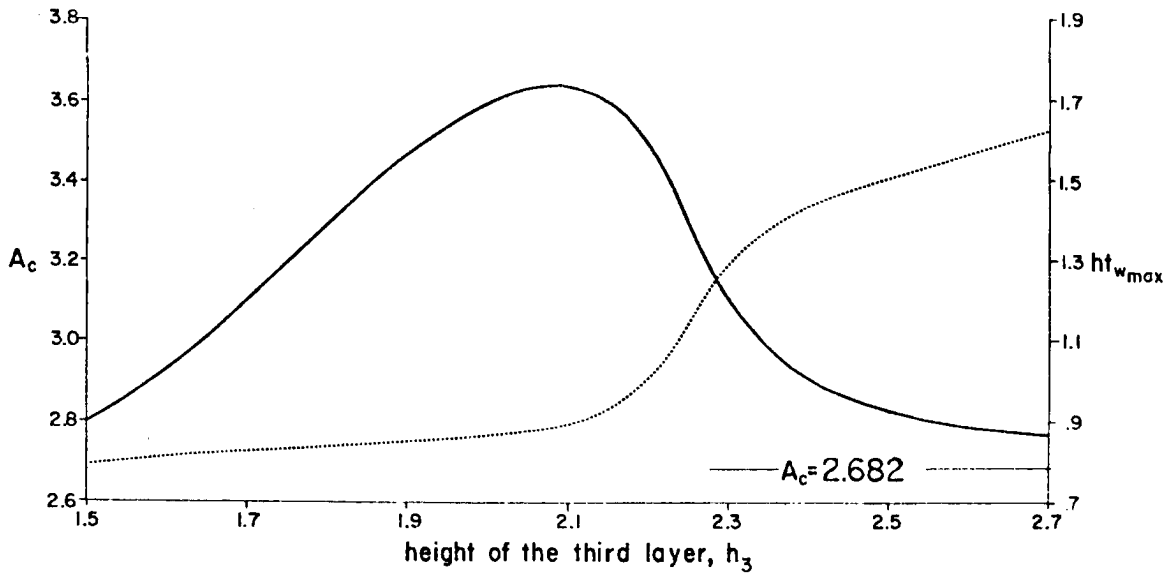
Fig. 5. Critical wave number (solid), A_c, and height of maximum vertical velocity, $ht_{w_{max}}$, versus height of the third layer, h_3.

B.2. The Thickness of the Middle Layer is Varied.

Table 3. Parameters defining the system of Part B.2.

Interface i	ϵ_{α_i}	ϵ_{β_i}	ϵ_{K_i}	ϵ_{ν_i}	ϵ_{ρ_i}	Layer i	h_i
2	1	-1.35	1	1	1	1	1
3	1	(a) .001	1	1	1	2	variable
	1	(b) .090	1	1	1	3	$5 \times h_2$
	1	(c) .180	1	1	1		

Thermal boundary condition: perfectly conducting boundaries, $\gamma \longrightarrow \infty$.

Table 4. Critical Rayleigh and wave numbers, for various values of ϵ_{β_3}, versus the thickness of the middle layer, d_2.

d_2	$\epsilon_{\beta_3} = .001$		$\epsilon_{\beta_3} = .090$		$\epsilon_{\beta_3} = .180$	
	R_c	a_c	R_c	a_c	R_c	a_c
0	64.982	.6616	170.548	1.3138		
.100	146.237	.7530	283.846	1.5432	335.949	1.7050
.129	229.071	1.0826				
.130	232.379	1.0986				
.131	235.691	1.1147				
.200	417.389	1.8299	440.635	1.9100	455.965	1.9550
.300	505.158	2.0455	508.795	2.0718	510.914	2.0789
.400	511.880	2.0503	516.675	2.0893	518.478	2.1006
.500	517.701	2.0901	519.289	2.1020	520.920	2.1038

Part B.1. demonstrates the effect of the upper boundary and forced convection upon the stability of the fluid in a system where the inversion is stable and the top layer is very unstable. However, in the atmosphere the fluid above the temperature inversion probably never has a temperature gradient as unstable as the layer bordering the ground. For this reason, in Part B.2., the third layer is made almost neutrally stable relative to layers one and two. The effect of the stability of the third layer is considered in this part and three different ϵ_{β_3} are used: $\epsilon_{\beta_3} = .001$, .090 and .180. The gravitational stability of the second layer relative to the first is slightly greater in Part B.2. ($\epsilon_{\beta_2} = -1.35$) than in Part B.1. ($\epsilon_{\beta_2} = -1.00$). The system is homogeneous throughout except for variations in temperature gradient.

In Part B.2., the effect of increasing the thickness of the middle layer is examined. As the middle layer increases in thickness it expands into the lowest layer. In Fig. 7, the height of the second layer is shown as $h_2 = 1.00$ for clarity, however, R_c and a_c are still scaled relative to the lowest layer: $h_1 = 1.00$.
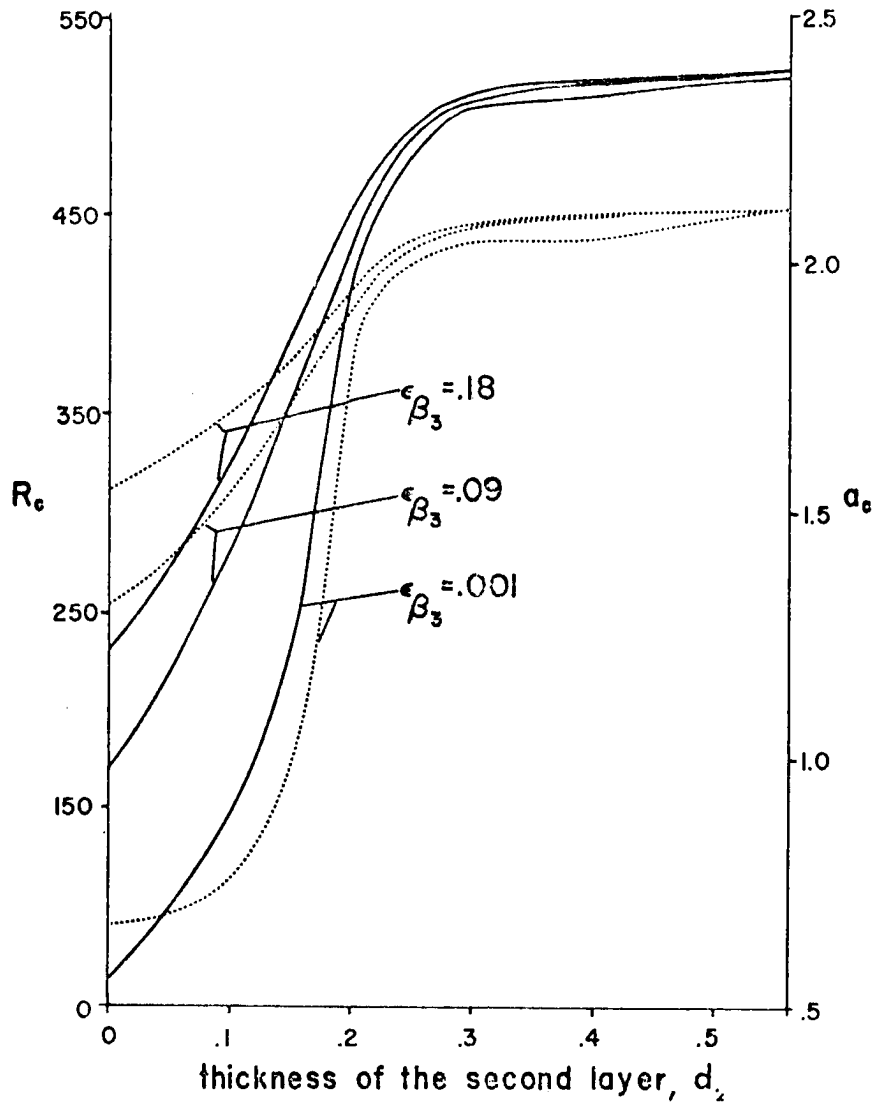

Fig. 6. Critical Rayleigh number (solid), R_c, and critical wave number (dotted), a_c, versus thickness of the middle layer, d_2.

Fig. 6 shows the critical Rayleigh and wave numbers versus d_2 for the three values of ε_{β_3}. As expected, R_c increases as the middle stable layer gradually occupies a larger proportion of the fluid. At first R_c increases at an increasing rate with increasing d_2 but this trend reverses for larger d_2 with the inflection point at $d_2 = .130$ for $\varepsilon_{\beta_3} = .001$. Inspection of the W and T' profiles shows that the inflection point occurs as the height of maximum vertical velocity approaches the top of the middle layer (Fig. 7 a, b and c). As the region of maximum vertical velocity enters the stable layer and then is confined below it (Fig. 7 d, e, f and g), R_c increases less rapidly with d_2 and finally approaches a limit. A factor which continues to stabilize the system and thus increase R_c, after $ht_{W_{max}}$ falls below the temperature inversion, is the advent of forced convection. The effect of forced convection in the upper layers on R_c, the Rayleigh number of the lowest layer, has already been discussed in Part B.1.

As d_2 continues to increase, a secondary cell of descending fluid forms above the cell of ascending fluid (Fig. 7 e, f and g). Convection in this secondary cell is free since W and T' are positively correlated (WT'>0). The reason for the formation of a second cell in the vertical is unknown. No reason for this is cited in the literature.
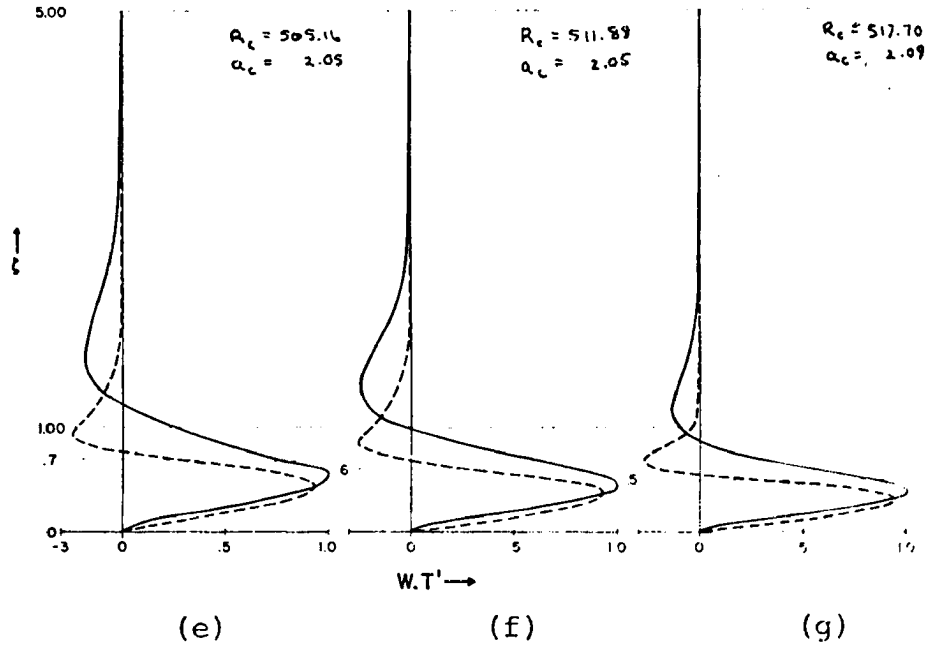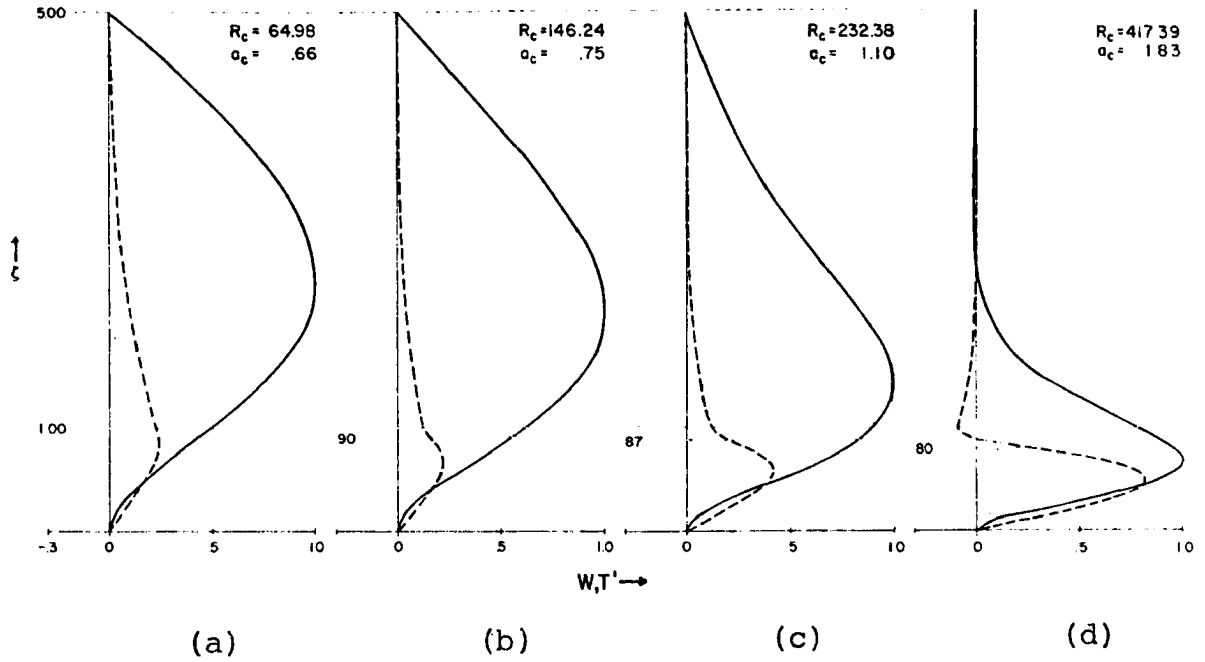
Fig. 7. Vertical velocity (solid), W, and temperature perturbation (dashed), T', for various thicknesses of the middle layer. Interfaces are shown by horizontal dashed lines.

Again, the dependence of the critical wave number upon
the parameter being varied, d_2, is very similar to that for
R_c. In fact the inflection points for R_c and a_c both occur
at the same value of d_2. As was observed in Part A, when
the region of maximum vertical velocity is confined to the
lowest layer, below the temperature inversion, a_c remains
essentially constant.

The effect of the stability of the third layer is evi-
dent in this second part of the investigation. R_c and a_c
are observed to be highly dependent upon the stability of
third layer before the thickness of the third layer becomes
a factor. However, as the middle layer becomes thicker,
providing a stable barrier to convective motions from the
lowest layer, the effect of the weak stability of the third
layer becomes insignificant by comparison.

C. In a Three Layer System, the Thermal Boundary Condition
   at the Lower Surface is Varied.

Table 5. Parameters defining the system of section 2.

Interface i	ϵ_{α_i}	ϵ_{β_i}	ϵ_{K_i}	ϵ_{ν_i}	ϵ_{ρ_i}	Layer i	h_i
2	1	−1.35	1	1	1	1	1.00
3	1	.001	1	1	1	2	1.43
						3	7.14

Thermal boundary condition: perfect conductor at top, $\gamma_T \longrightarrow \infty$;
perfect conductor to perfect insulator at bottom, $\gamma_B \rightarrow \infty$ to $\gamma_B \rightarrow 0$.

Table 6. Critical Rayleigh and wave numbers for various values of Biot number, γ_B, at the bottom boundary.

γ_B	R_c	a_c
10^5	505.158	2.0454
10^3	504.738	2.0449
10	471.419	1.9850
1	382.359	1.7395
10^{-1}	332.033	1.5313
10^{-2}	323.984	1.4920
10^{-6}	323.030	1.4872

In the atmosphere, convective cells similar to those observed by Bénard in liquids are often observed by meteorological satellites over the ocean below subsidence inversions (Kruger and Fritz, 1961). However, theory and actual observation do not agree in some respects. One difference is that the predicted horizontal dimension of this convective cell is about 1/10 that observed in the atmosphere. Two physical properties of the atmosphere, not included in classical convection theory, may cause this. One of these is the anisotropy of the eddy coefficients of viscocity and thermal conductivity in the atmosphere (Priestly, 1962, Palm, 1960, and Ray and Scorer, 1963). Further discussion of this phenomena is deferred to Part D. The second property involves the thermal boundary condition. The boundaries in the atmosphere are probably not perfect conductors of infinite heat capacity as prescribed in the classical theory but are to some degree insulating (Sparrow, Goldstein and

Johnson, 1964, and Sasaki, 1970). The effect of the thermal

boundary condition at the lower surface will be examined in

this part.

The fluid system being considered in this section is

the same as one considered in the previous part, defined by

Table 3, except for the thermal boundary condition, with

d_2 = .3, and shown in Fig. 7 e. The thermal boundary condi-

tion, given by equation (44), at the upper surface is that of

a perfect conductor where $\gamma_T \to \infty$. At the lower surface, the

Biot number, γ_B, in equation (41) ranges from 10^{-6} to 10

which corresponds to the lower boundary going from a nearly

perfect insulator to a nearly perfect conductor.

To begin the discussion of this part, we consider the

effect of γ_B on the critical Rayleigh and wave numbers. Fig.

8 shows that R_c and a_c are both fairly insensitive to chang-

ing γ_B for very large or very small values of γ_B but changes

rapidly as γ_B goes from 10^{-2} to 10^2. The same result was

found by Sparrow et al. for a one layer fluid with rigid-

rigid, rigid-free, and free-free dynamic boundary conditions.

The most stable situation occurs for large γ_B where both the

upper and lower boundaries approximate a perfect conductor

of infinite heat capacity. This is expected, intuitively,

since the conducting boundaries allow much of the heat in

the lowest part of the system to be conducted away through

the lower boundary and convection is not necessitated. The

vertical velocity and temperature profiles for the most the

stable situations, corresponding to $\gamma_B = 10^5$, 10^3 and 10,

are shown in Fig. 7 e and Fig. 9 a and b. It is noted that
the temperature perturbation is zero or very small at the
lower boundary for these cases because any temperature devi-
ation from the mean temperature at the boundary is largely
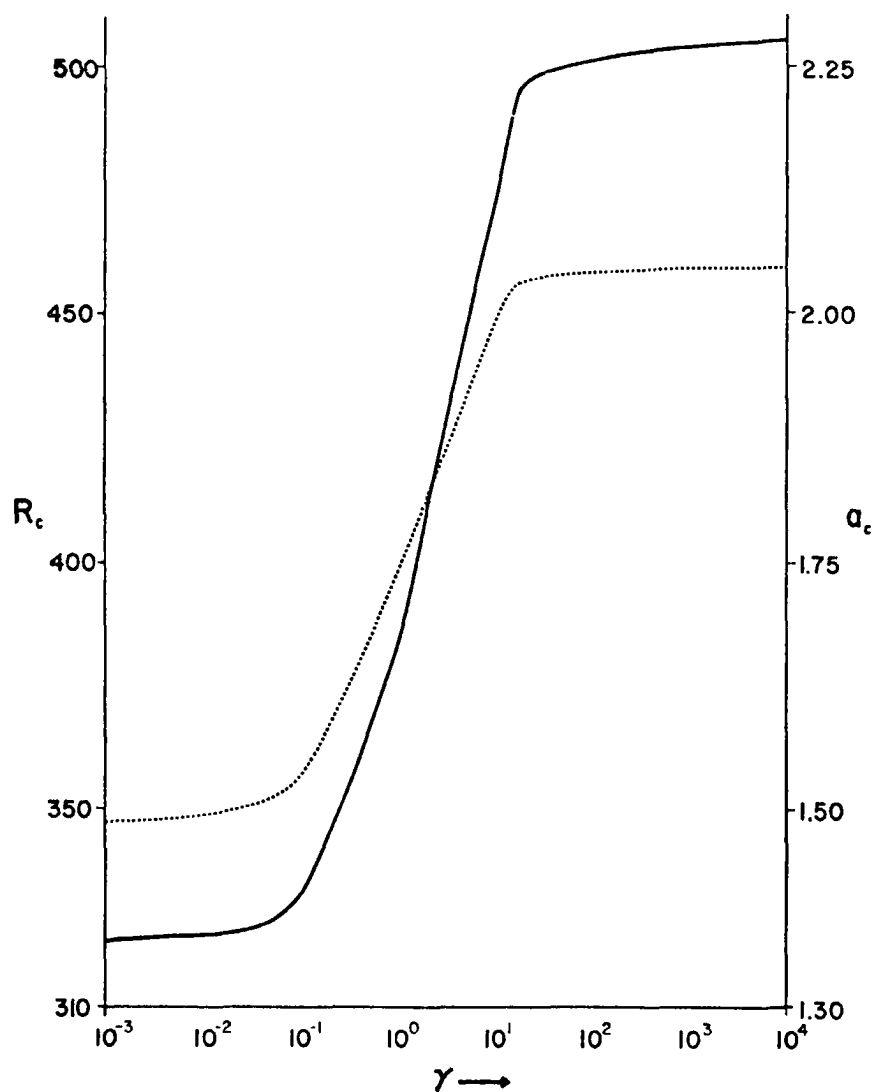conducted away by the boundary.

Fig. 8. Critical Rayleigh number (solid), R_C, and critical
wave number (dotted), a_c, versus Biot number, γ_B of
the lower boundary.

That the system is more unstable when the lower bound-
ary is an insulator also seems reasonable since, for this
case, a temperature deviation from the mean cannot be con-
ducted away through the boundary and the system must go to
convection to dissipate this temperature excess. The more
unstable situations, for which γ_B = .1, 10^{-2} and 10^{-6}, are
shown in Fig. 9 c, d, e and f. The temperature perturbation
is seen to increase gradually as the lower boundary becomes
more insulating.

A limiting value of R_c occurs for very large values of
γ_B because the lower boundary assumes the properties of a
good conductor for $\gamma_B \approx 10$. Beyond that the conductivity of
the boundary increases only slightly. For example, the tem-
perature perturbation at ζ = 0 for γ_B = 10^3 (Fig. 9 a) is
close to zero. The temperature perturbation for γ_B = 10^5
(Fig. 7 e) at ζ = 0 may be half that for γ_B = 10^3 but is
still essentially zero with respect to characteristic values
of temperature perturbations in the fluid. Similarly, for
γ_B = 10^{-1} the lower boundary is a good insulator and DT',
which is proportional to the perturbation heat flux, is al-
most zero. For $\gamma_B < 10^{-1}$, DT' decreases but is still zero
with respect to characteristic values of DT' within the
fluid. The transition between the two limiting values of R_c
occurs when the lower boundary is neither a good conductor
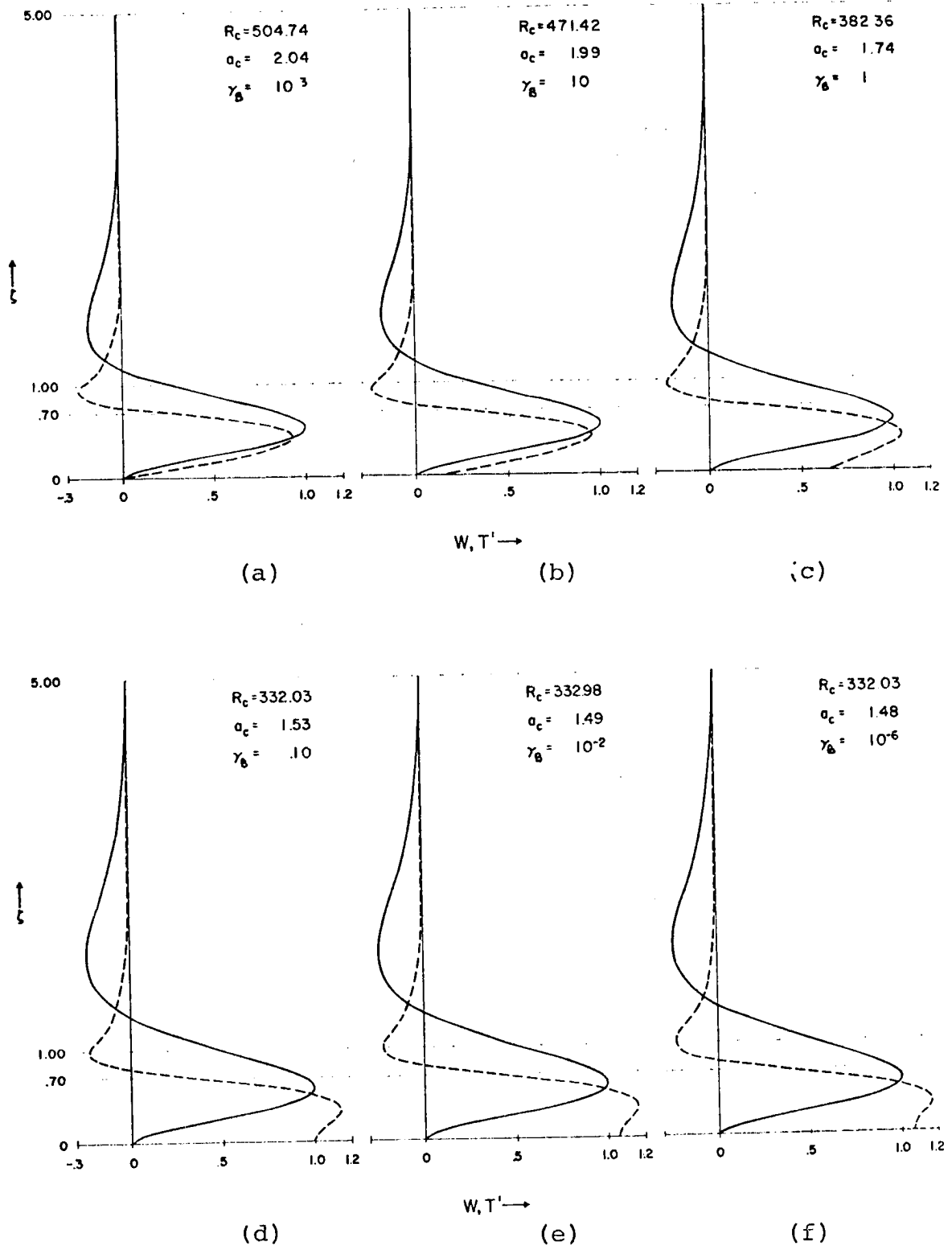nor a good insulator.

Fig. 9. Vertical velocity (solid), W, and temperature per-
         turbation (dashed), T', for various values of Biot
         number, γ_B, at the lower boundary. Interface are
         shown by horizontal dashed lines.

Inspection of Fig. 10 provides further evidence of the
fluid being more unstable for lower γ_B. Fig. 10 shows WT'
versus ζ for three values of γ_B when the rate of viscous
dissipation of kinetic energy $(\propto (D^2-a^2)W)$ integrated over
the depth of the fluid is normalized for each γ_B. It can be
seen for the most unstable case, $\gamma_B = 10^{-6}$, a smaller rate
of release of internal energy in the lowest layer is neces-
sary for convective overturning to begin. This is expected
since R_c is smaller for $\gamma_B = 10^{-6}$ then for $\gamma_B = 1$ or 10^3.
It can also be seen that when the lower boundary is an insu-
lator the rate of release of internal energy in the lowest
part of the fluid is greater and less kinetic energy is lost
to forced convection.

The less restrictive thermal boundary condition does
indeed result in flattening of the convective cells and thus
probably better approximates the atmospheric thermal bound-
ary condition. However in the limit $\gamma_B \to 0$, for which the
convective cells in the system being considered here attain
their maximum horizontal extent, the ratio of the vertical
to horizontal extent of the lowest cell is only ~1/4 which
is still far from what is observed in the atmosphere (~1/10).
The reason for this is that here we require the convective
motion to penetrate not only the lowest layer but the top
two inversion layers while in the atmosphere convection is
usually confined to the lowest unstable region. This means
that a larger amount of energy must be released in the low-
est, unstable, layer here and transferred upward in order to

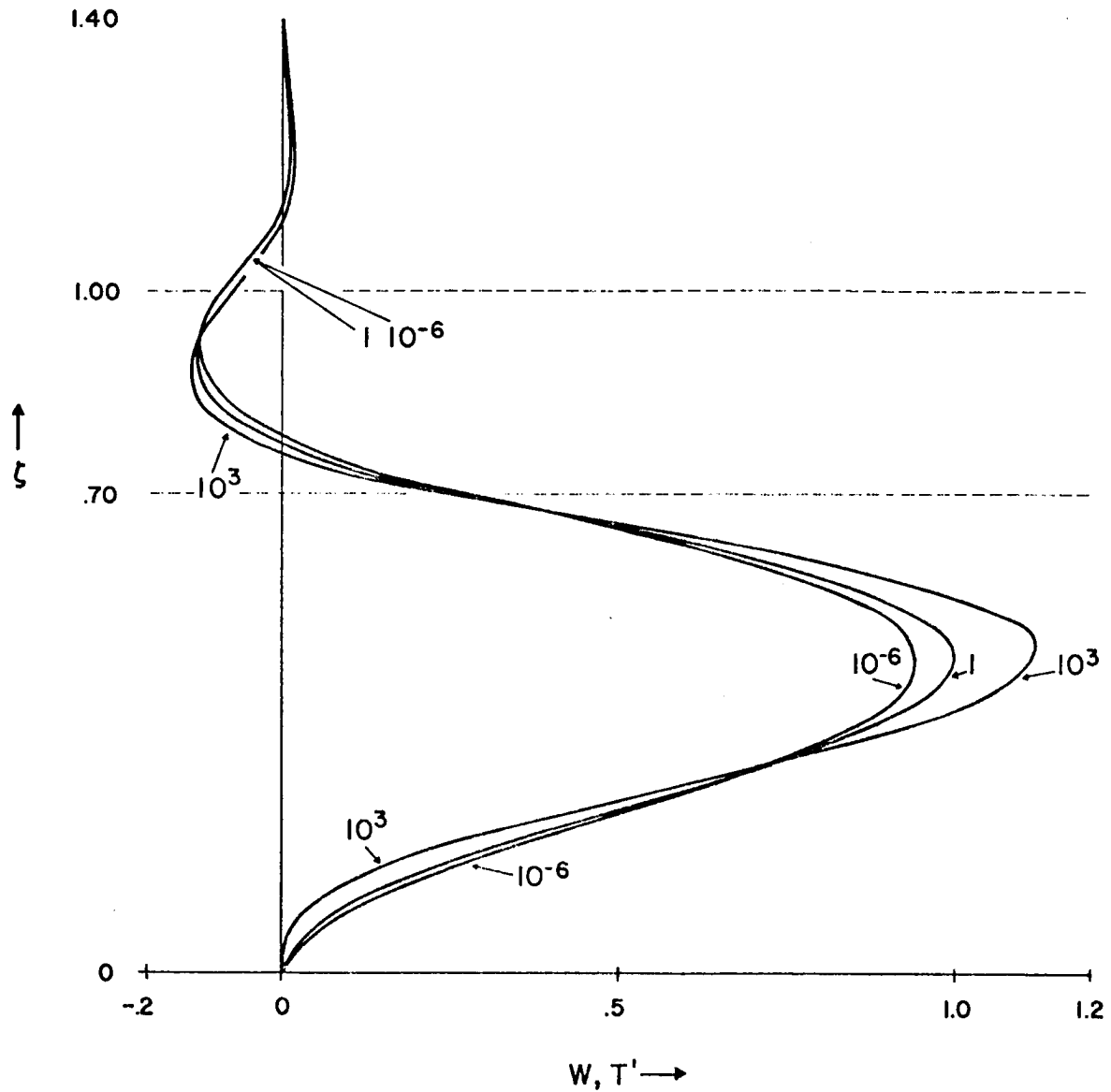Fig. 10. Rate of release of internal energy ($\propto WT'$) for various values of Biot number, γ_B.

penetrate the top two stable layers than in the atmospheric case. It seems reasonable that this larger energy transfer from the bottom to the top of the fluid in the present case is more efficiently accomplished by a greater density per unit volume of weak cells than by a large, strong cell.

D. In a Four Layer System, the Conductivity and Viscosity of the Second Layer Above the Ground are Varied.

Table 7. Parameters defining the system of Part D.

Interface i	ϵ_{α_i}	ϵ_{β_i}	ϵ_{K_i}	ϵ_{ν_i}	ϵ_{ρ_i}	Layer i	h_i
2	.985	-.001	variable	$=\epsilon_{K_2}$	.944	1	1.00
3	1.000	1.000	$1/\epsilon_{K_2}$	$=\epsilon_{K_3}$	1.000	2	36.55
4	1.003	20.000	.1	.1	.921	3	148.00
						4	150.00

Thermal boundary condition: perfect conductor at top, $\gamma_T \longrightarrow \infty$; good insulator at bottom, $\gamma_B \longrightarrow 6.27 \times 10^{-4}$.

Table 8. Critical Rayleigh and wave numbers versus ε_{K_1} (or ε_{ν_1}). R_c in this case corresponds to the local minimum R occurring at the lowest a, $a_c = a(R_c)$.

$\epsilon_{K_2}(or \epsilon_{\nu_2})$	R_c	a_c
1	130.497	.1102
10	130.148	.1099
25	485.282	.1048
40	934.390	.1079
55	1419.912	.1145
72	1969.449	.1395

In the third, and final part, the vertical anisotropy of the thermal conductivity and kinematic viscosity are modeled by stepwise vertical variation of these parameters. In the classical system, the fluid is homogeneous with respect to the various convection parameters; the molecular coefficients of thermal conductivity and kinematic viscosity

are constant throughout the system. However, in the atmos-
phere, the Reynolds number is so high that molecular proces-
ses are of little importance and eddy transport processes
must be considered. One would expect, therefore, the magni-
tude of these eddy diffusion coefficients to be roughly pro-
portional to the magnitude of the velocity field. In this
section, these coefficients have been varied vertically in
four steps according to the magnitude of the vertical veloc-
ity by using a four layer system.

Four layers are the result of modeling the system after
the trade wind inversion. One layer is required to simulate
the shallow, unstable layer just above the ocean surface.
It has a thickness of 10 to 100 m. Above this is a deep,
slightly stable layer of approximately 1500 m with the
stable trade wind inversion above it. Assuming the convec-
tive motion penetrates the lowest two layers and enters a
small distance into the inversion, the system requires three
layers to describe the convection. The vertical velocity
profile was found for this three layer system and a fourth
layer was introduced to contain the region of maximum verti-
cal velocity which occurred throughout approximately the
lower one-third of the second layer.

Maximum values of K and ν are then assigned to this new
layer. The actual values of the eddy diffusion coefficients
for the atmosphere are not well established but it is thought
they may be one or two orders of magnitude larger in the
region of maximum convection than in other parts of the

fluid (Faller and Kaylor, 1970 and Deardorff, 1967). The relative magnitudes of K and ν in the first, third and fourth layers are held constant and the effect of varying K and ν in the second layer is examined. In all cases the Prandtl number, $P \equiv K/\nu$, for each layer is equal to one.

In an effort to model the real atmospheric mean temperature and density structure, the values of $\alpha (= \frac{1}{T_m})$ and ρ_m are not held constant from one layer to another but given values of a characteristic trade wind temperature inversion. For example, since the lowest layer is strongly heated it has a mean temperature greater than that of the layer above it and $\varepsilon_{\alpha_2} = .985$. Due to the compressibility of the atmosphere the lowest layer has the greatest density and $\varepsilon_{\rho_2} = .944$. At the lower surface, the thermal boundary condition of $\gamma_B = 6.27 \times 10^{-4}$ is used, as suggested by Sasaki. The thermal boundary condition at the upper boundary is that of a perfect conductor, $\gamma_T \to \infty$.

Looking first at Fig. 11, it can be seen that R_c increases monotonically with ε_{K_2} and ε_{ν_2}. This is expected since larger viscosity in the second layer serves to increasingly damp out the buoyant motions generated by the lowest layer. Also, larger conductivity of the second layer allows heat to be transferred to the upper part of the fluid by conduction and a larger temperature difference between top and bottom of the system is required for convection. Thus, the fluid becomes more stable for higher values of ε_{K_2} and ε_{ν_2}.
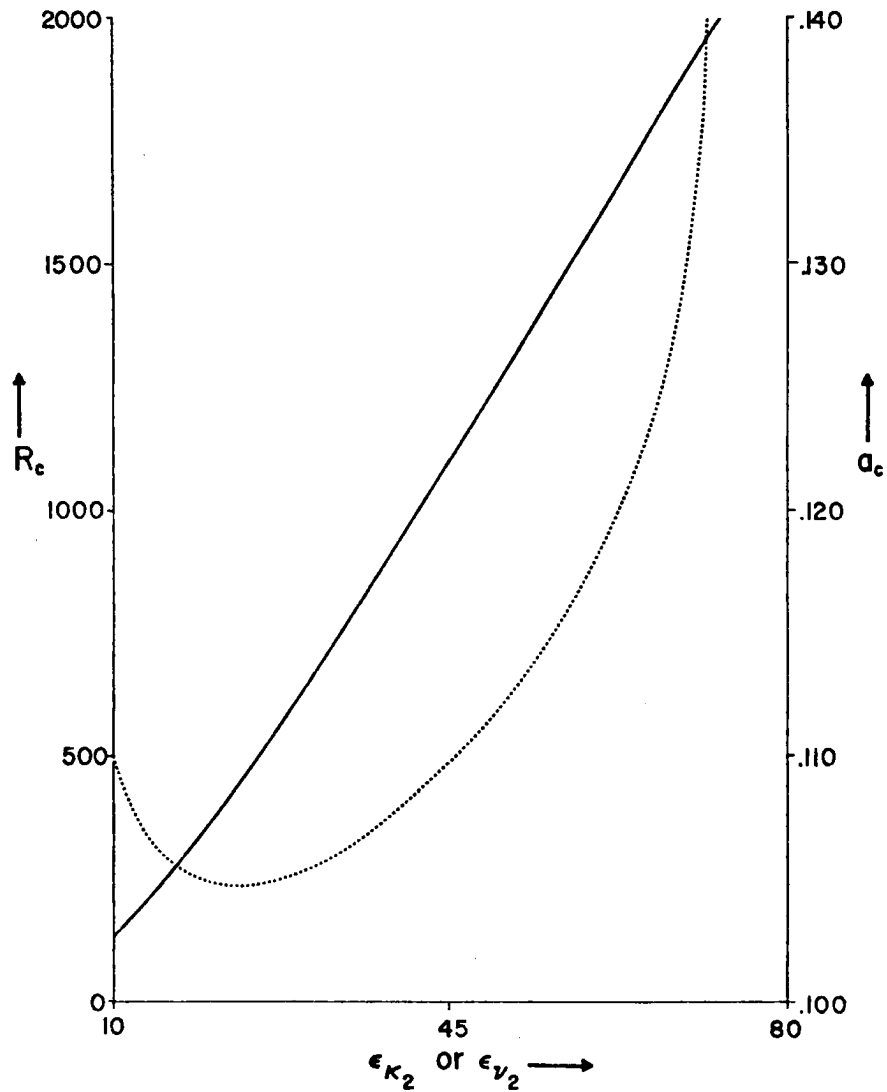
Fig. 11. Critical Rayleigh number (solid), R_C, and critical
wave number (dotted), a_C, versus the ratio of
thermometric conductivity (or equivalently the
ratio of kinematic viscosity) between layers two
and one.

The critical wave number clearly behaves much differ-
ently in Fig. 11 than what we have seen in the previous two
sections. R_c and a_c react almost independently to changing
ε_{K_2} and ε_{v_2}. R_c increases monotonically but a_c decreases

reaching a minimum at $\varepsilon_{K_2} = 22.5$ (or equivalently ε_{ν_2}) and then goes asymptotic to $\varepsilon_{K_2} = 72$. An explanation of this behavior of a_c can be found by examining Fig. 12 which shows Rayleigh number versus wave number for increments of ε_{K_2} of 15. Fig. 11 is a plot of the first (left) local minimum R and the corresponding a. These appear to be the critical Rayleigh and wave numbers for the type of gravitation instability which was studied in the previous parts. Fig. 12 shows that another minimum occurs for large values of ε_{K_2} and ε_{ν_2} at higher wave numbers. The unusual behavior of a_c in Fig. 11 is probably due to an interaction between the two instabilities.

This second type of instability is probably similar to that discussed by Welander (1964) although some important differences exist between Welander's model and the present one. Welander's two layer model demonstrates that a type of convective instability can exist, even when the fluid is heated from above, if the thermal expansion coefficient and conductivity are larger in one layer than in the layer bordering it. Referral to Table 7 shows that this condition does exist at interfaces two and four. However, differences between the present model and Welander's should be noted. In Welander's system the interface is not deformed by the fluid motions since an interface boundary condition $W_i = W_{i+1} = 0$ is assumed whereas the present model uses $W_i = W_{i+1}$ where W_i is not necessarily zero. Thus, the two models differ in this respect but it is still probable that the second

instability which occurs here is related to the discontinuities in α and K at interfaces 2 and 4.
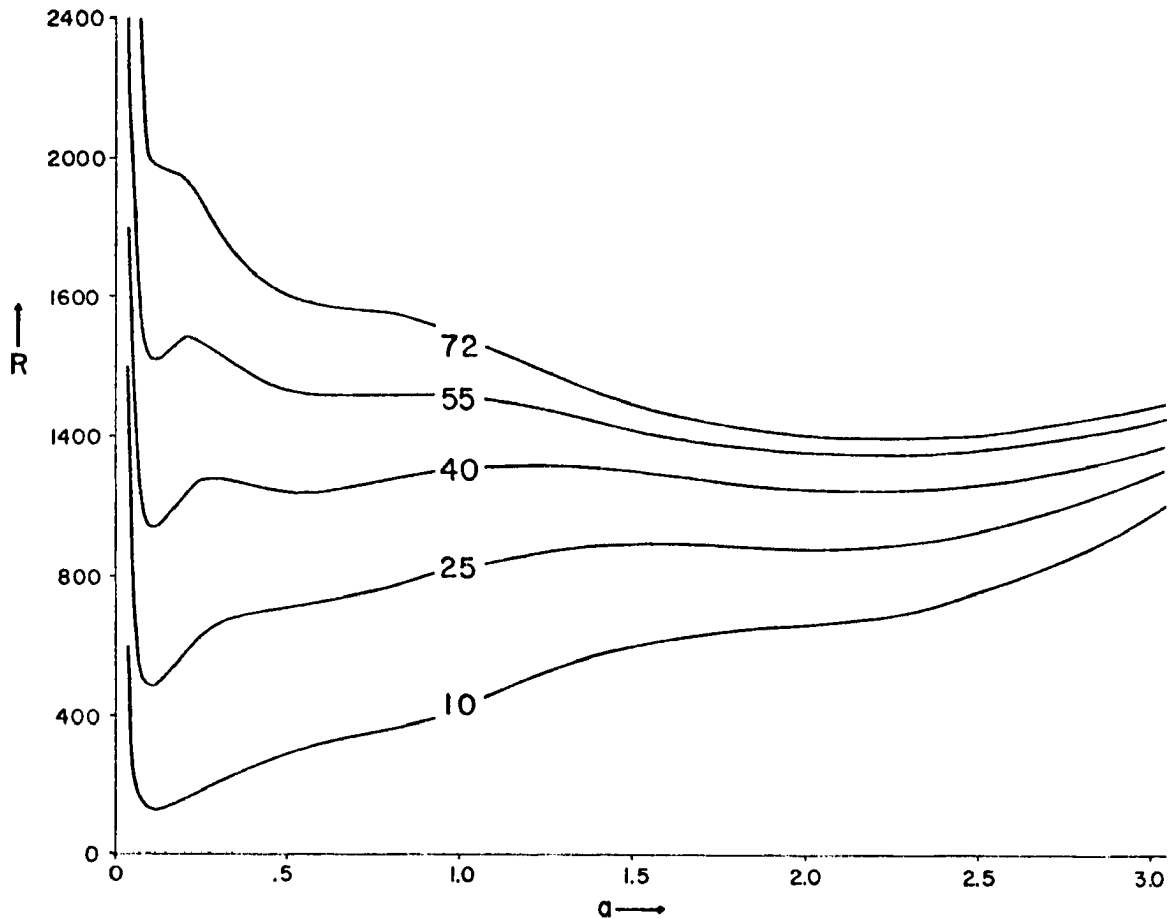

Fig. 12. Rayleigh number versus wave number for various values of the ratio of thermometric conductivity between layers two and one.

Fig. 13 shows the W and T' profiles for several values of ε_{K_2}. The vertical velocities have not been normalized because, graphically, no difference between the four profiles could then be seen. It can be seen that the maximum velocity field still occurs in the second layer--even for large values of ε_{K_2} and ε_{V_2}. A weak second cell is observed to form just

above the second layer but it probably does not significantly affect the stability of the system since T' is essentially zero in this region and, thus, the magnitude of the rate of buoyant release of energy in this region is relatively small. W and T' are both effectively zero above $\zeta = 50$. It is indeed observed in the atmosphere (Malkus, 1952) that convective motion below a trade wind inversion does not usually penetrate to the height of the inversion unless the ascending fluid gains additional buoyancy due to condensation and the release of latent heat. Only dry convection is considered in this model.
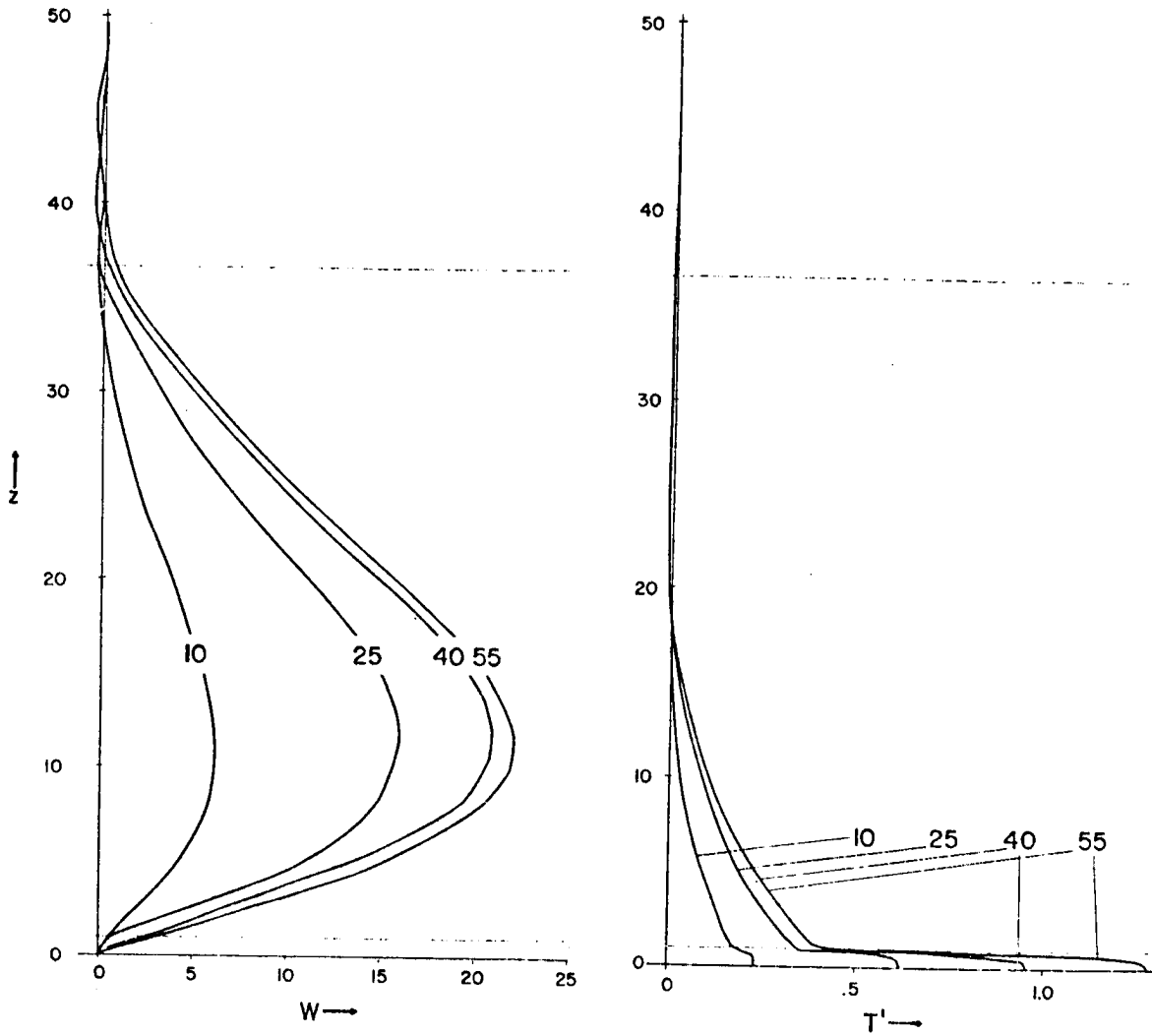
Fig. 13. Vertical velocity, W, and temperature perturbation, T', for various values of thermometric conductivity between layers two and one. Interfaces are shown by horizontal dashed lines.

VI.   SUMMARY AND CONCLUSIONS

An analytical model has been developed which describes
convection for the case of marginal stability in a fluid of
N layers.   In general, each layer may have a different ther-
mal expansion coefficient, temperature gradient, thermometric
conductivity, kinematic viscosity, and density.   The bound-
aries of the system may separately range from being a per-
fect conductor to a perfect insulator.

Several problems occur in seeking the minimum Rayleigh
number for the lowest mode wave number, i.e., the critical
Rayleigh number, and in finding an eigenfunction which satis-
fies all boundary conditions.   An eigenvalue, R, at a given
wave number, a, is found by successive estimates of R such
that the coefficient determinant of the solution is a mini-
mum.   The eigenvalue, R, can be found to an accuracy of 10
to 11 digits at a given "a" but this is sometimes not accurate
enough to insure an eigenfunction which satisfies all the
boundary conditions.   The computer could be programmed to
find R to twice this number of significant digits however
such a program would require a large amount of computer time,
however no other solution to this problem has been found.   A
second problem is that of finding the true critical Rayleigh
number.   The curve for R versus a is very broad in the
region of the minimum Rayleigh number and, because of this,

it is difficult to find the true minimum R to more than $\pm 10^{-7}$%.

The model is applied to a number of different fluid systems and several general properties of the free convective mode become evident. If the configuration of the fluid is such that a second cell in the vertical forms, the stability of the systems tends to increase if in the region of the second cell the temperature perturbation is essentially zero. The reason for this is that the second cell supplies none of its own energy but must be driven by the primary cell. Thus an increased rate of release of internal energy in the lowest unstable part of the fluid is required for convective overturning to take place. The second cell may act to destabilize the fluid if the vertical velocity and temperature perturbation of the second layer are positively correlated. Internal energy is then also released in the second layer. This reduces the rate of release of internal energy in the lower part of the fluid necessary to produce convective motions which penetrate the fluid since the second cell, at least partially, drives itself. Forced convection (WT'<0) stabilizes the fluid because some of the internal energy released in the lower part of the fluid is stored in the form of potential energy in the region of forced convection. Thus, not all of the internal energy released goes to kinetic energy to penetrate the fluid and the rate of release of internal energy must increase for convection to occur.

The thermal boundary condition affects the stability of the system. If the lower boundary assumes the properties of a conductor, energy released in the lower part of the fluid can be conducted away through the lower boundary and the fluid is relatively stable. Conversely, if the lower boundary is an insulator, the fluid is less stable and the transition from the conductive mode of heat transfer to convective occurs at a smaller temperature gradient since little energy goes out through the lower boundary.

The usual type of convective instability does not occur when the fluid layers are not all of the same thermometric conductivity and thermal expansion coefficient. The instability which occurs in this case is probably similar to that found by Welander who showed that convective instability can occur even in a fluid heated from above when the thermal expansion coefficient and the conductivity are large in one layer and small in the other.

In general, the horizontal wave number depends upon the stability of the fluid. For less unstable configurations of the fluid a small horizontal cell size is the most efficient in transferring energy from the lower part of the fluid. For more unstable configurations, the horizontal density of cells is greater.

Several improvements over the present model could be made. Nondimensionalization of the mean state temperature field would allow a more complete heat flux interface boundary condition. In the present model, the ratios of the

Rayleigh numbers at the interfaces between layers, given by the ϵ_i^1, ϵ_i^2 and ϵ_i^3, are held fixed. However the Rayleigh numbers themselves are not fixed. For easier application to the atmosphere it would be useful to fix the Rayleigh numbers of the upper layers and vary only the Rayleigh number of the lowest layer.

REFERENCES

REFERENCES

Calder, K. L., 1968: In clarification of the equations of shallow-layer thermal convection for a compressible fluid based on the Boussinesq approximation. *Quart. J. R. Meteor. Soc.*, 94, 88-92.

Chandrasekhar, S., 1961: *Hydrodynamic and Hydromagnetic Stability*. Oxford University Press.

Deardorff, J. W., 1967: Empirical dependence of the eddy coefficient for heat upon stability above the lowest 50 m. *J. Appl. Meteor.*, 6, 631-643.

Faller, A. J., and R. Kaylor, 1970: Numerical studies of penetrative convective instabilities. *J. Geophys. Res.*, 75, 521-530.

Gribov, V. N., and L. E. Gurevich, 1957: On the theory of the stability of a layer located at a superadiabatic temperature gradient in a gravitational field. *Sov. Phys. JETP*, 4, 720-729.

Krueger, A., and S. Fritz, 1961: Cellular cloud patterns revealed by TIROS I, *Tellus*, 13, 1-7.

Malkus, J. S., 1952: Recent advances in the study of convective clouds and their interaction with the environment. *Tellus*, 4, 71-87.

Mihaljan, J. M., 1962: A rigorous exposition of the Boussinesq approximation applicable to a thin layer of fluid. *Astrophys. J.*, 136, 1126-1133.

Ogura, Y., and H. Kondo, 1970: The linear stability of convective motion in a thermally unstable layer below a stable region. *J. Meteor. Soc. Japan*, 48, 204-215.

Palm, E., 1960: On the tendency toward hexagonal cells in steady convection. *J. Fluid Mech.*, 8, 183-192.

Priestly, C. H. B., 1963: Width-height ratio of large convective cells. *Tellus*, 14, 123-124.

Ray, D., and R. S. Scorer, 1963: *Studies of the problems of cellular convection in the atmosphere.* Final Report, U.S. Weather Bureau Contract cwb - 10004.

Sasaki, Y., 1967: Influences of the thermal boundary layer on atmospheric cellular convection. *J. Meteor. Soc. Japan,* 48, 492-501.

Sparrow, E. M., R. J. Goldstein, and V. K. Jonsson, 1964: Thermal instability in a horizontal fluid layer: effect of boundary conditions and non-linear temperature profile. *J. Fluid Mech.,* 18, 513-528.

Spiegal, E. A., and G. Veronis, 1960: On the Boussinesq approximation for a compressible fluid. *Astrophys, J.,* 131, 442-447.

Stix, M., 1970: Two examples of penetrative convection. *Tellus,* 22, 517-520.

Welander, P., 1964: Convective instability in a two-layer fluid heated uniformly from above. *Tellus,* 16, 349-358.